THE "NET" IMPACT OF HYDROTHERMAL VENTING ON OCEANIC ELEMENTAL INVENTORIES

CONTRIBUTIONS TO PLUME GEOCHEMISTRY FROM THE INTERNATIONAL GEOTRACES PROGRAM

By Jessica N. Fitzsimmons and Janelle M. Steffen

A high-temperature hydrothermal vent field discovered on Puy des Folles Seamount on the Mid-Atlantic Ridge, at approximately 2,000 meters (6,562 feet) in depth, during the In Search of Hydrothermal Lost Cities expedition. *Image courtesy of Schmidt Ocean Institute*

ABSTRACT. Hydrothermal vents serve as a primary interface between the cold deep ocean and the warm oceanic crust. While early research showed that seawater-rock interactions add to or remove elements from seawater during the generation of hydrothermal fluids, consideration of these fluid fluxes alone does not relay the total impact that hydrothermal systems have on seawater geochemistry. In addition, hydrothermal plumes, areas where hydrothermal fluids mix with ocean waters, are host to a range of particle precipitation and scavenging reactions that further modify gross hydrothermal fluid fluxes to define the total "net" hydrothermal impact on oceanic inventories. Here, we review the major discoveries made by the international GEOTRACES program regarding the geochemical transformations occurring within hydrothermal plumes. We classify each element into one of five categories based on its behavior in hydrothermal plumes, a spectrum spanning the geochemical mass balance between net hydrothermal source fluxes and net hydrothermal plume scavenging sinks. Overall, we celebrate the role that GEOTRACES has played in defining the extent and dynamics of hydrothermal plume geochemistry, which is a crucial lever for determining global hydrothermal impacts.

INTRODUCTION

Hydrothermal venting occurs when seawater permeating through fissures in the oceanic crust is geothermally heated, driving water-rock reactions that modify the chemical composition of the permeating seawater, creating hydrothermal fluids. Due to their high temperatures, which can at times exceed 300°–400°C, hydrothermal fluids are buoyant and rise upward through the crust into the ocean. The best studied high-temperature hydrothermal vents, which occur along mid-ocean ridges at divergent tectonic plate boundaries, release fluids that are acidic, anoxic, metal-rich, and magnesium (Mg)-free (Von Damm et al., 1985). These vent fluids also precipitate copious iron (Fe)- and manganese (Mn)-rich particles upon mixing with cold, oxygenated deep-ocean seawater, which gives plumes their canonical "black smoker" appearance (Mottl and McConachy, 1990).

Since the discovery of hydrothermal vents in 1977 (Corliss et al., 1978; Spiess et al., 1980), high priority has been given to understanding the influence of hydrothermal venting on the geochemical inventories of elements in the ocean. In fact, by studying the geochemistry of the altered basalt on the seafloor, oceanographers were able to predict what the chemical composition of hydrothermal fluids might be before they were even discovered (Humphris and Thompson, 1978). Additionally, the oceanic mass balances of several elements could not be resolved without the discovery of hydrothermal fluids (Mackenzie and Garrels, 1966), including Mg, which famously had a "missing sink" flux from the ocean that was eventually discovered to be dominated by Mg precipitation into crustal rocks during hydrothermal water-rock interactions (Humphris and Thompson, 1978). Quickly upon the discovery of low-temperature Galápagos hydrothermal vents in 1977 (Corliss et al., 1978), the elemental composition of the Galápagos fluids were correlated to their heat flux and extrapolated to the global geothermal heat flux for an estimation of global hydrothermal fluxes, which were shown to be sufficiently large to rival or even exceed global riverine fluxes (Edmond et al., 1979). Hydrothermal vents were found to be major sources to the ocean of at least lithium (Li), rubidium (Rb), sulfate, calcium (Ca), potassium (K), barium (Ba), silica (Si), and Mn. When high-temperature vents were discovered a few years later (Spiess et al., 1980), the same elemental-heat correlations produced similar extrapolated hydrothermal fluid concentrations (Edmond et al., 1982).

In the two decades after Edmond and coauthors' initial global hydrothermal flux estimates, there were at least two additional attempts at global hydrothermal flux calculations that incorporated newer hydrothermal research into their estimates (Elderfield and Schultz, 1996; Alt, 2003). Critically, both of these studies acknowledged that using only hydrothermal fluid concentrations to calculate the impact of hydrothermal venting on seawater elemental inventories allows only a "gross" estimate of hydrothermal fluxes. The role of subsequent elemental transformations within hydrothermal plumes (Figure 1)—defined here as the neutrally buoyant, laterally extending mixtures of dilute hydrothermal fluids, their associated suspended particles, and entrained seawater that can extend thousands of kilometers into the ocean—was mentioned but purposefully excluded from the flux calculations of these seminal hydrothermal flux studies, largely due to lack of complete knowledge of plume dynamics. The abundant Fe- and Mn-rich particles in hydrothermal plumes were known to adsorb, aggregate, and/or co-precipitate dissolved elements from the hydrothermal fluids and/or the plume's entrained seawater in a process collectively known as scavenging (Kadko et al., 1995). Thus, the total impact of hydrothermal venting on the geochemical mass balance of the ocean (Figure 1) is:

"gross" flux (from hydrothermal fluids) ± modifying plume fluxes = "net" impact on oceanic inventory.

Here, we celebrate and review the role that the international GEOTRACES program has played in revealing the chemical transformations that occur in hydrothermal plumes (Figure 1, Table 1). We emphasize that it is not the "gross" chemical fluxes from buoyant hydrothermal fluids that set the total impact of hydrothermal activity on the ocean's elemental inventories but rather the "net" influence, which also includes significant elemental scavenging that occurs in hydrothermal plumes.

GEOCHEMISTRY OF BUOYANT HYDROTHERMAL FLUIDS: THE "GROSS" CHEMICAL FLUX TO THE OCEAN

The global hydrothermal flux syntheses published at the turn of the century (Elderfield and Schultz, 1996; Alt, 2003) advanced our understanding of hydrothermal impacts on ocean chemistry in two important ways. First, both used improved estimates of hydrothermal heat flux, calculated using multiple quantification methods (Kadko et al., 1995), for the global extrapolation. Second, Alt (2003) added estimates of low-temperature ridge-flank chemical alteration to the high temperature gross chemical fluxes of prior calculations, although the fluid chemistry of these ridge flanks remained poorly constrained. The two flux calculations agreed that hydrothermal fluids are sources to the ocean of alkali metals, beryllium (Be), Ca, Ba, boron (B), Si, sulfide, metals, and magmatic volatiles, and they are sinks from the ocean of Mg, sulfate, alkalinity, and phosphorus (P). Importantly, however, both studies admitted one major shortcoming of their calculations: they purposefully ignored the more opaque chemical transformations occurring in hydrothermal plumes.

Hydrothermal fluid research over the subsequent two decades has also revealed that these prior global flux studies were further limited by the fact that their gross hydrothermal flux calculations employed only concentrations from canonical "high-temperature black smoker" vents at mid-ocean ridges (Von Damm, 1995). Instead, we now understand there to be a large diversity in the temperature and chemical composition of hydrothermal vent fluids (reviewed in German et al., in press). In fact, it is said that no two hydrothermal vents have the same fluid composition. For example, we have discovered that hydrothermal circulation occurs across extremely varied geotectonic settings, including mid-ocean ridges, volcanic arcs, back-arcs, subduction zones, and intra-plate volcanic hotspots, all with different fluid geochemistry (reviewed in German et al., in press). This has allowed an improved focus on the role of source rock geochemistry in setting vent fluid chemical composition. For example, while canonical "black smoker" studies were conducted in regions hosted by mafic crustal rocks, more recent studies of slow and ultra-slow spreading ridges have shown the participation of ultramafic mantle rocks in hydrothermal water-rock interactions that exhibit unique fluid geochemistry (Kelley et al., 2005), including the presence of serpentinization reactions (Charlou et al., 2010). Altogether, multiple factors are also thought to control overall hydrothermal fluid chemistry, including geologic setting (including spreading rate and source rock), maximum temperature and pressure of the fluid in the subsurface, extent of fluid phase separation, extent of magmatic degassing, extent of mixing with seawater in the subseafloor aquifer, presence and

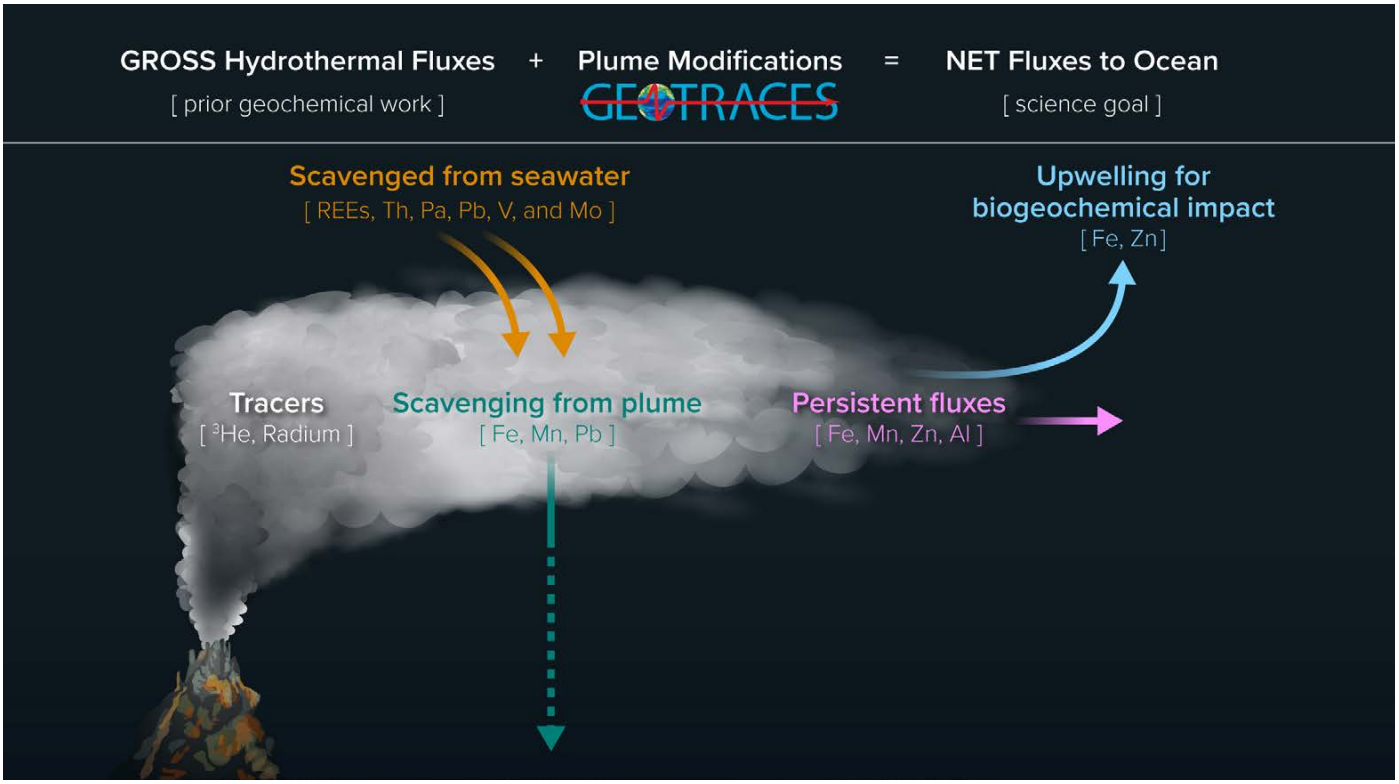

FIGURE 1. GEOTRACES research has transformed our understanding of elemental behavior in hydrothermal plumes, understanding that is critical to any assessment of the "net" hydrothermal impact on oceanic elemental inventories. GEOTRACES studies have provided insights into how to trace plume dilution and mixing, the rates and mechanisms of elemental scavenging onto particles from both seawater and hydrothermal fluid enrichments themselves, and the extent and impact of persistent hydrothermal fluxes to the open ocean.

TABLE 1. Summary of GEOTRACES studies of hydrothermal plume geochemistry, by element, categorized by dissolved elemental behavior in plumes. Acronyms for common vent fields are used, including the East Pacific Rise (EPR), Juan de Fuca Ridge (JdFR), Mid-Atlantic Ridge (MAR), Southern East Pacific Rise (SEPR), and Trans-Atlantic Geotraverse (TAG) vent fields.

GEOTRACES CONTRIBUTIONS TO HYDROTHERMAL PLUME STUDIES			
ELEMENT	**ENRICHED OR SCAVENGED IN THE PLUME?**	**ESTIMATED FLUXES & RESIDENCE TIMES**	**REFERENCES**
TRACERS			
He	^{3}He plumes have been detected 500 km away from the MAR (1), 4,000 km away from the SEPR (2,3,5), as well as distally from both JdFr (5) and Kama'ehuakanaloa (4,5)		(1) Jenkins et al., 2015 (2) Lupton and Jenkins, 2017 (3) Jenkins et al., 2018 (4) Jenkins et al., 2020 (5) Jenkins et al., 2023
Ra	Ra anomalies have been observed in the TAG (1), SEPR (2), Reykjanes (3), and Kermadec arc (4) plumes		(1) Charette et al., 2015 (2) Kipp et al., 2018 (3) Le Roy et al., 2018 (4) Neuholz et al., 2020b
SCAVENGED FROM SEAWATER			
Cd	dCd removal reported in MAR plume (11–77 pmol kg^{-1}), likely from Fe oxyhydroxides (1)		(1) Conway and John, 2015
Mo	dMo depletions and pMo enrichments near the SEPR axis, scavenged by both Fe and Mn oxides (1)	dMo hydrothermal removal rate = 10^{7} mol yr^{-1} (1)	(1) Ho et al., 2018
Pa	Both TAG (1) and SEPR (2) vent plumes show clear trends of dPa depletion (as far as 4,000 km off axis), with depletion being 30%–70% of background values (2)		(1) Hayes et al., 2015a (2) Pavia et al., 2018 (3) Gdaniec et al., 2020
Pb	dPb in hydrothermal vents shows mixed behavior, with scavenging of anthropogenic dPb also observed at the MAR (1,2) and EPR (3,4)		(1) Noble et al., 2015 (2) Rigaud et al., 2015 (3) Niedermiller and Baskaran, 2019 (4) Boyle et al., 2020
REE	Lau Basin (1), TAG (2), and SEPR (4) showed clear depletions in rare earth element (REE) concentrations (10%–60% deficits from background); however, there was less evidence of REE depletions in Arctic plumes (3)	dNd hydrothermal removal rate = 3.44 x 10^{6} mol yr^{-1} (2)	(1) Behrens et al., 2018 (2) Stichel et al., 2018 (3) Paffrath et al., 2021 (4) Basak et al., 2024
Th	Substantial ^{230}Th depletions are observed at TAG (1), Arctic Nansen Basin (3,5), and the SEPR as far as 4,000 km away from the ridge axis (2,4). Non-zero but small hydrothermal source of ^{232}Th is also present (3)	Depletion timescales for ^{230}Th from hydrothermal plumes = 64 yr (2)	(1) Hayes et al., 2015a (2) Pavia et al., 2018 (3) Valk et al., 2018 (4) Pavia et al., 2019 (5) Gdaniec et al., 2020
V	dV depletions and pV enrichments near the SEPR axis, scavenged mostly by Fe oxyhydroxides (1)	dV hydrothermal removal rate = 10^{9} mol yr^{1} (1)	(1) Ho et al., 2018
MIXED BEHAVIOR IN HYDROTHERMAL PLUMES			
Co	Small, localized sources of dCo shown near the SEPR (1), MAR (2), and Kama'ehuakanaloa (4); however, no dCo source was shown near JdFR (3), and hydrothermal dCo scavenging was also observed more distally (1,4)	dCo hydrothermal flux from Kama'ehuakanaloa = 6 ± 3 x 10^{4} mol yr^{-1} (4)	(1) Hawco et al., 2016 (2) Noble et al., 2017 (3) Zheng et al., 2019 (4) Chmiel et al., 2022
Cu	The plume above the MAR in the North Atlantic was shown to be a net sink for dCu (1,2), there seemed to be no hydrothermal influence on dCu in the South Atlantic (3), and there was a very low elevated concentration of dCu (4) and Cu ligands (5) along the SEPR		(1) Jacquot and Moffett, 2015 (2) Roshan and Wu, 2015a (3) Little et al., 2018 (4) Roshan and Wu, 2018 (5) Ruacho et al., 2020
LOCAL HYDROTHERMAL FLUX			
Ac	Elevated activities of ^{227}Ac were observed at the TAG vent field (1) and in the surrounding North Atlantic (2), attributed to hydrothermal origin	^{227}Ac hydrothermal flux calculated to be 1.9%–5.8% of sediment flux for the Atlantic (1)	(1) Kipp et al., 2015 (2) Le Roy et al., 2023
Ba	No dBa enrichments in TAG or SEPR plumes (1), but small dBa anomaly and light δ^{138}Ba isotope anomaly points to a tiny hydrothermal contribution near Gakkel Ridge, Central Arctic (2)		(1) Rahman et al., 2022 (2) Whitmore et al., 2022
Cr	dCr contributions from the Kermadec Arc are small but present in Southern Ocean data (1), 8–27 nmol kg^{-1} above background levels	dCr hydrothermal flux from the Kermadec Arc = 10 to 10^{4} mol yr^{-1} (1)	(1) Janssen et al., 2023
Ga	Small but noticeable source of dGa surrounding the SEPR (1), up to 35 pmol kg^{-1} compared to background	dGa global hydrothermal flux = 8.6 ± 1.7 × 10^{6} mol yr^{-1} (1)	(1) Ho et al., 2019

Table continued...

TABLE 1. Continued...

GEOTRACES CONTRIBUTIONS TO HYDROTHERMAL PLUME STUDIES			
ELEMENT	**ENRICHED OR SCAVENGED IN THE PLUME?**	**ESTIMATED FLUXES & RESIDENCE TIMES**	**REFERENCES**
LOCAL HYDROTHERMAL FLUX – continued...			
Hg	Total dHg and MMHg is elevated near the TAG hydrothermal vent (1) and along the MAR generally (3), but no total dHg enrichment was observed along the SEPR (2)	Total Hg hydrothermal flux from mid ocean ridges = 1.5–64.7 tons yr^{-1} (4)	(1) Bowman et al., 2015 (2) Bowman et al., 2016 (3) Bratkič et al., 2016 (4) Torres-Rodriguez et al., 2024
Si	Small dSi enrichments above the SEPR (2) and Gakkel Ridge (3), but TAG and other SEPR show no concentration change (1,2)		(1) Brzezinski and Jones, 2015 (2) Grasse et al., 2020 (3) Liguori et al., 2020
PERSISTENT HYDROTHERMAL FLUX			
Al	Elevated concentrations of dAl are observed at the MAR (2) and up to 3,000 km away from the SEPR (3,4), but are not observed in Arctic plumes (1,5)	dAl global hydrothermal flux = $6.1 \pm 2.4 \times 10^9$ mol yr^{-1} (6) dAl hydrothermal residence time = 156 yr (6)	(1) Middag et al., 2009 (2) Measures et al., 2015 (3) Resing et al., 2015 (4) Ho et al., 2019 (5) Measures and Hatta, 2021 (6) Xu and Weber, 2021
Fe	Various GEOTRACES studies have shown elevated dFe concentrations associated with hydrothermal plumes. The most extreme case shows dFe elevation up to 4,300 km from the ridge axis. dFe hydrothermal inputs have been observed in the Southern Ocean (1,14–15,24,29), the Arctic Ocean (2,27,30,34), the MAR (4–7,9,11,22–23,26,33,35–36), the Indian Ocean (3,8,19,31), the SEPR (10,12–13,16–17,25), the Caribbean (20–21), the Southwest Pacific (27,33), and along the JdFR (37)	dFe hydrothermal residence time = 9–50 yr (18) or 21–31 yr (32)	(1) Klunder et al., 2011 (2) Klunder et al., 2012 (3) Nishioka et al., 2013 (4) Saito et al., 2013 (5) Conway and John, 2014b (6) Rijkenberg et al., 2014 (7) Fitzsimmons et al., 2015 (8) Gamo et al., 2015 (9) Hatta et al., 2015 (10) Resing et al., 2015 (11) Sedwick et al., 2015 (12) Fitzsimmons et al., 2016 (13) Fitzsimmons et al., 2017 (14) Klar et al., 2017 (15) Lough et al., 2017 (16) Buck et al., 2018 (17) John et al., 2018b (18) Kipp et al., 2018 (19) Chinni et al., 2019 (20) Lough et al., 2019a (21) Lough et al., 2019b (22) Pagnone et al., 2019 (23) González-Santana et al., 2020 (24) Holmes et al., 2020 (25) Roshan et al., 2020 (26) Tonnard et al., 2020 (27) Cohen et al., 2021 (28) Gerringa et al., 2021 (29) Sieber et al., 2021 (30) Zhang et al., 2021 (31) Chinni and Singh, 2022 (32) Tagliabue et al., 2022 (33) Tilliette et al., 2022 (34) Wang et al., 2022 (35) Hoffman et al., 2023 (36) Lough et al., 2023 (37) Chan et al., 2024
Mn	dMn was elevated in hydrothermal plumes as far as 500 km from the MAR (1,3), the Gakkel Ridge (4,8), and in the Gulf of Aden (2), and as far as 3,000 km off the SEPR (5), as well as along the Kermadec Arc (7) and JdFR (9)		(1) Wu et al., 2014 (2) Gamo et al., 2015 (3) Hatta et al., 2015 (4) Middag et al., 2015 (5) Resing et al., 2015 (6) González-Santana et al., 2020 (7) Neuholz et al., 2020a (8) Gerringa et al., 2021 (9) Chan et al., 2024
Zn	Persistent dZn enrichments were observed at TAG (1, 2), 4,000 km downstream of the SEPR (3,5), and 1,000 km from the Reykjanes Ridge (4)	dZn global hydrothermal flux = $1.75 \pm 0.35 \times 10^9$ mol y^{-1} (3)	(1) Conway and John, 2014a (2) Roshan and Wu, 2015b (3) Roshan et al., 2016 (4) John et al., 2018a (5) Lemaitre et al., 2020

composition of sediments above the venting site, and rates of microbial activity within the fluids prior to venting.

This recently discovered variety in the chemical composition of hydrothermal fluids makes extrapolation of gross hydrothermal fluxes to the global ocean particularly challenging. However, comparisons of fluid properties within and across vent fields are made easier by data mining, including the incredible MARHYS (MARine HYdrothermal Solutions) vent fluid database created by Diehl and Bach (2020), which promises exciting future syntheses across hydrothermal vent types globally. Nevertheless, modern research on vent distributions and fluid geochemistry continues, especially focusing on the global extent and chemical composition of vents at slow and ultraslow spreading centers, as well as the under-explored, low-temperature diffuse flow vents that surround axial vents (Bemis et al., 2012; Lough et al., 2019a), all of which are important vent systems whose distribution across the global ocean and fluid chemical compositions remain poorly constrained.

GEOCHEMISTRY OF HYDROTHERMAL PLUMES: THE CRITICAL ROLE OF GEOTRACES RESEARCH

The previously published calculations of global hydrothermal fluxes (Edmond et al., 1979; Elderfield and Schultz, 1996; Alt, 2003) focused on gross hydrothermal fluid fluxes but were not able to calculate for the full suite of elements the additional chemical fluxes occurring within hydrothermal plumes, due to both a lack of knowledge of the global extent of hydrothermal plumes and analytical challenges in measuring low elemental concentrations within plumes. The first of these was overcome by investigations of metalliferous sediment distributions (Boström et al., 1969) and global analyses of the distal plume tracer helium (^{3}He) (Lupton and Craig, 1981; Jenkins et al., 2019). The second was overcome by technological advancements and the rigorous analytical methods, standardization, and intercalibration motivated by the expectations of the international GEOTRACES program (Aguilar-Islas et al., 2024, in this issue).

Nonetheless, by the mid-1990s it was acknowledged that the mixing of hot, anoxic, and metal-rich fluids with cold, oxygenated seawater results in the precipitation of copious Fe- and Mn-rich particles (Mottl and McConachy, 1990), which facilitate the scavenging removal of surface-active dissolved elements from seawater in hydrothermal plumes (reviewed in Kadko et al., 1995; Lilley et al., 1995). Careful study of plume particulate metal concentrations suggested several mechanisms for dissolved metal loss (German et al., 1991), including (1) co-precipitation with Fe oxyhydroxides such as for the oxyanions arsenic (As), chromium (Cr), and vanadium (V); (2) precipitation with sulfide particles for chalcophilic elements such as copper (Cu), zinc (Zn), and lead (Pb); and (3) adsorption onto Fe- and Mn-rich particle surfaces for surface-active elements such as the rare earth elements (REEs) and Be. From dissolved element measurements, there was also a growing understanding that deep ocean dissolved phosphate, an oxyanion, could be net removed from the ocean by adsorption onto or co-precipitation with Fe- and Mn-oxides (Feely et al., 1990). Together, these studies boldly suggested that, for some elements, hydrothermal venting might, in fact, not be a net source to the ocean at all, as gross hydrothermal sources to the ocean could be equaled or exceeded by scavenging sinks within hydrothermal plumes (German et al., 1991).

Since then, research from the international GEOTRACES program has revolutionized our understanding of chemical transformations within hydrothermal plumes. The GEOTRACES Science Plan (GEOTRACES Planning Group, 2006) identified hydrothermal vents as one of four major external interfaces of the ocean, and thus GEOTRACES cruises have prioritized the study of chemical transformations between hydrothermal fluids and the ocean interior within plumes. The US GEOTRACES GP16 Eastern Pacific Zonal Transect specifically targeted the 4,000 km-long Southern East Pacific Rise (SEPR) plume, previously identified by metalliferous sediment (Boström et al., 1969) and oceanic ^{3}He distributions (Lupton and Craig, 1981), offering a major advancement in our understanding of the extent, timescale, and mechanisms of hydrothermal plume fluxes occurring over wide spatial scales. In contrast to work at the fast-spreading SEPR, the HERMINE (GApr07) and FRiDGE (GA13) GEOTRACES expeditions focused on hydrothermal plumes on the slow-spreading Mid-Atlantic Ridge. Finally, many other GEOTRACES transects and process studies have investigated hydrothermal plumes from a variety of tectonic settings (Table 1) and produced valuable plume discoveries (see visual impacts of hydrothermal plumes on GEOTRACES elemental sections in Conway et al., 2024, in this issue).

Here, we review GEOTRACES studies of hydrothermal plumes, and we split elements into five categories based on their plume behavior (Table 1): (1) elements behaving conservatively and serving as chemical tracers in hydrothermal plumes, (2) elements net scavenged from plumes and/or deep-ocean seawater, (3) elements with mixed behavior in different hydrothermal plumes, (4) elements with "local" hydrothermal fluxes that do not extend far from the vent source, and (5) elements with persistent hydrothermal fluxes reaching far into the open ocean. In essence, these five categories span the spectrum of the balance between net hydrothermal fluid source fluxes and net hydrothermal plume scavenging sinks.

1. Tracer Elements. First, GEOTRACES studies made exemplary use of ^{3}He, the quintessential conservative tracer (not scavenged or biologically cycled) for hydrothermal plume mixing (e.g., Resing et al., 2015). Even on a qualitative basis, GEOTRACES utilized ^{3}He as the ideal chemical fingerprint of hydrothermal

influence when identifying the provenance of deep-sea dissolved metal anomalies (e.g., Saito et al., 2013; Jenkins et al., 2020; Lough et al., 2023). In fact, the global hydrothermal ^{3}He flux (modeled in Bianchi et al., 2010) as a function of ridge spreading rate has been combined with measured plume dissolved Fe/^{3}He ratios to predict global hydrothermal Fe fluxes to the ocean (Tagliabue et al., 2010). GEOTRACES studies were also the first to measure radium (Ra) isotopes in distal hydrothermal plumes (Charette et al., 2015) that, when combined with conservative ^{3}He, were used to calculate hydrothermal plume ages at individual plume locations (Kipp et al., 2018). In fact, combinations of the ^{3}He and Ra isotope tracers allowed scavenging-derived nonconservations in dissolved Fe distributions to be identified and quantified within hydrothermal plumes (Fitzsimmons et al., 2017; Kipp et al., 2018).

2. Scavenged Elements. A second major advancement made by GEOTRACES hydrothermal plume research was the study of dissolved elements that are net removed from seawater by scavenging onto hydrothermal Fe- and Mn-rich particles (Table 1). While this research confirmed the elemental groupings of scavenging-type elements originally proposed by German et al. (1991), it more importantly added substantial detail on the spatial extent, magnitude, rates, and chemical drivers of particle scavenging in hydrothermal plumes, whose rates for some elements rival or even exceed the better-studied boundary scavenging rates occurring along high-productivity ocean margins. For example, for the oxyanions, study of high-resolution sampling data along the 4,000 km-long SEPR plume showed that dissolved phosphate, V (present in seawater as $H_2VO_4^-$), and molybdenum (Mo, present in seawater as MoO_4^{2-}) are net scavenged from seawater, mostly near the ridge axis, with dissolved-phase depletions concomitant with particulate enrichments (Ho et al., 2018). Additionally, GEOTRACES size partitioned correlations between particulate V or Mo with particulate Fe and Mn confirmed that pV is primarily scavenged by Fe oxyhydroxides, while pMo could be scavenged by both Fe- and Mn-oxides (Ho et al., 2018).

In contrast to the oxyanions, which show relatively small (<10%) depletions from large deep ocean dissolved inventories, GEOTRACES global surveys illuminated massive deficits of REEs, thorium (Th), and protactinium (Pa) from abyssal seawater inventories in hydrothermal plumes from diverse geotectonic settings all over the globe (Table 1). These deficits range from 10% to 60% of abyssal inventories of REEs (Behrens et al., 2018; Stichel et al., 2018; Paffrath et al., 2021) to 30% to 70% of abyssal ^{230}Th and ^{231}Pa (Hayes et al., 2015a; Pavia et al., 2018, 2019; Valk et al., 2018; Gdaniec et al., 2020). GEOTRACES analyses also showed that the radiotracers ^{230}Th and ^{231}Pa are particularly valuable in quantifying partition coefficients that translate scavenging rates onto different particle types, which have revealed hydrothermal ^{230}Th scavenging onto predominantly Fe oxyhydroxides and ^{231}Pa scavenging onto Mn oxides (Hayes et al., 2015a; Pavia et al., 2018). This partitioning is important for predicting metal scavenging in hydrothermal plumes with relatively more/fewer of these particles, such as at the Trans Atlantic Geotraverse (TAG) hydrothermal system, which is relatively Mn oxide-poor compared to other vent systems (Trocine and Trefry, 1988), or at different portions of the SEPR plume, which are variably dominated by particulate Mn or Fe at different depths (Fitzsimmons et al., 2017; Lee et al., 2018). A similar partition coefficient approach was used to show that REEs such as neodymium (Nd) are scavenged onto both Fe- and Mn-oxides in plumes (Stichel et al., 2018), with evidence for greater relative adsorption onto Mn oxides closer to the ridge axis but greater continued adsorption onto Fe (oxyhydr)oxides downplume (Basak et al., 2024).

A multi-radiotracer approach was also used to verify that Th isotopes are continually scavenged onto hydrothermal particles downplume (Pavia et al., 2019), which is different from the oxyanions that are mostly scavenged near the ridge axis (Ho et al., 2018). This also may explain why the oxyanions have linear particulate metal/Fe trends, while the REEs (and Th and Pa) have particulate metal/Fe trends curved upward, connoting their continuous scavenging from seawater along the plume's length (German et al., 1991).

Finally, dissolved Pb was confirmed to be net scavenged from seawater, despite its >10^6x enrichments in hydrothermal fluids above abyssal concentrations (Table 1; MARHYS database, Diehl and Bach, 2020). Pb, alongside Cu and Zn, form a group of "chalcophilic" (sulfur-loving) elements that are thought to co-precipitate with Fe sulfides and be net-scavenged from hydrothermal plumes (German et al., 1991). GEOTRACES Pb isotope studies have been particularly useful in studying the balance of hydrothermal fluid Pb sources versus seawater scavenging sinks. For example, Boyle et al. (2020) showed that even though EPR vent fluid Pb concentrations represent a gross source flux to seawater, the removal of Pb by scavenging onto ferromanganese-rich particles in the SEPR plume is so significant that only 1% of the basaltic Pb signatures could be identified isotopically. Similarly, the REEs and ^{232}Th can be enriched above seawater in vent fluids due to hydrothermal water-rock reactions (MARHYS database); GEOTRACES research has revealed both inert colloidal ^{232}Th enrichments along the SEPR plume (Pavia et al., 2018) and mild but unique Nd isotopic signatures directly above the TAG and SEPR ridges (Stichel et al., 2018; Basak et al., 2024). However, net hydrothermal processes (fluids + plume) act as a net sink of these elements from the ocean.

3. Elements with Mixed Hydrothermal Plume Behavior. The third group of elements studied by GEOTRACES contains Cu and cobalt (Co), which uniquely show hydrothermal enrichments in some plumes and scavenging deficits in others

(Table 1). The MARHYS database shows that Cu and Co can both be enriched in hydrothermal fluids in >10^5x abyssal dissolved concentrations, magnitudes that might otherwise point to a major hydrothermal source flux to the oceans. However, Cu is also a "chalcophilic" scavenging-type element that is strongly scavenged in hydrothermal plumes by sulfide precipitation and/or scavenging onto ferromanganese particles (German et al., 1991), while hydrothermal Co scavenging is often associated with Mn oxides (Moffett and Ho, 1996; van Hulten et al., 2017). Thus, the excess or deficit of dissolved Cu or Co in global hydrothermal plumes depends on the detailed balance of its hydrothermal sources and sinks.

Source rock and metal:sulfide ratio in the vent fluids can certainly affect Cu precipitation from hydrothermal fluids, both in the buoyant plume and even subsurface during fluid transport, influencing the gross hydrothermal fluid Cu flux. However, GEOTRACES research revealed that the ability for electron-rich organic compounds called "ligands" to bind dissolved Cu cations in seawater, protecting it from scavenging, may also play an important role in setting ultimate hydrothermal Cu fluxes to the ocean (Sander and Koschinsky, 2011). Copper ligand concentrations at the TAG hydrothermal site were low (Jacquot and Moffett, 2015), contributing to local net dCu scavenging at TAG (Roshan and Wu, 2015a); however, Cu ligands were in greater excess of Cu in the SEPR plume (Ruacho et al., 2020), potentially contributing to the ~0.3 nM excess of hydrothermally derived dissolved Cu observed in the SEPR plume (Roshan and Wu, 2018). In contrast, GEOTRACES studies have revealed a source of labile ("free") Co^{2+} that is subsequently scavenged downplume because it is not stabilized by organic-Co-binding ligands. Thus, dissolved Co enrichments above background are small and are only present in hydrothermal plumes proximal to the TAG, SEPR, and Kama'ehuakanaloa (formerly Lō'ihi) vent sites, if they are enriched above background at all (Hawco et al., 2016; Noble et al., 2017; Chmiel et al., 2022). Sometimes dCo shows deficits at the ferromanganese oxide particle maximum in the hydrothermal plume, which occur when scavenging outcompetes the hydrothermal source (Hawco et al., 2016).

4. Elements with "Local" Source Fluxes. The fourth group of hydrothermal plume elemental behaviors revealed by GEOTRACES studies includes a range of elements—actinium (^{227}Ac), Ba, Cr, gallium (Ga), mercury (Hg), and Si—that never exhibit net scavenging but only have local dissolved enrichments in hydrothermal plumes proximal to the ridge axes that do not persist very far into the ocean interior (Table 1). There are two reasons these elements have only local hydrothermal enhancements. First, most of these elements—Ba, Cr, Ga, Hg, and Si—are only weakly enriched in vent fluids so when the fluids are diluted several orders of magnitude by seawater in the neutrally buoyant plume, the hydrothermal enrichment can hardly or cannot be distinguished from the abyssal ocean background (Ho et al., 2019; Rahman et al., 2022; Janssen et al., 2023; Torres-Rodriguez et al., 2024). Instead, isotopes of these elements have been utilized to detect hydrothermal anomalies, for example, δ^{138}Ba in the Arctic (Whitmore et al., 2022), δ^{53}Cr in the Kermadec Arc (Janssen et al., 2023), and δ^{30}Si at TAG and in the Arctic (Brzezinski and Jones, 2015; Liguori et al., 2020).

Another reason some of these elements have only local hydrothermal enrichments is subsequent loss to the particle phase, as for the partially scavenged Cu and Co described above, but perhaps to a lesser extent of scavenging. GEOTRACES sections indicate some evidence for both ^{227}Ac and Hg scavenging to ferromanganese particles (Kipp et al., 2015; Bowman et al., 2016; Le Roy et al., 2023), though this scavenging is insufficient to drive ^{227}Ac and Hg deficits below background concentrations. Finally, in the SEPR plume, Si exhibited complex concentration and isotopic patterns over short spatial scales near the ridge axis that cannot be explained without some Si precipitation as amorphous silica, quartz, or another secondary Si mineral close to the vents (Grasse et al., 2020). Thus, for these elements, low hydrothermal fluid abundances combined with high abyssal inventories and/or some scavenging drives only mild net excess source fluxes to the ocean.

5. Elements with Persistent Hydrothermal Fluxes. The hydrothermal plume elements best studied by the international GEOTRACES program—aluminum (Al), Fe, Mn, and Zn—all exhibit significant concentration excesses above abyssal backgrounds in long-distance hydrothermal plumes (Table 1, Figure 1). The >3,000 km-long hydrothermal enrichments of dissolved Al, Fe, and Mn in the SEPR plume, one of the highest-impact discoveries of the entire GEOTRACES program, famously made the cover of *Nature* (Resing et al., 2015), but these hydrothermal metal excesses are also found within many other GEOTRACES sections in every ocean basin, from the Arctic to the Pacific, Atlantic, and Indian Oceans, and all the way to the Southern Ocean (Table 1, and graphically captured across the global ocean by Conway et al., 2024, in this issue). The MARHYS database (Diehl and Bach, 2020) suggests that hydrothermal fluids can have up to 10^5x enrichments of Al and Zn and up to 10^7x enrichments of Fe and Mn compared to abyssal seawater. It is these large enrichments in hydrothermal fluid concentrations that provide the greatest chance for these elements to exhibit anomalies, even when diluted >10^4x by seawater in distal hydrothermal plumes (Lupton, 1995).

Surprisingly, of this group of metals, only dissolved Zn is not a scavenging-type element, as it is only thought to be mildly reversibly scavenged within seawater (John and Conway, 2014; Sieber et al., 2023). This explains why hydrothermal plume dZn excesses can persist >1,000 km from the Reykjanes Ridge in the subpolar North Atlantic (Lemaitre et al., 2020) and >3,000 km along the

SEPR plume (Roshan et al., 2016). This hydrothermal dissolved Zn can also be detected via isotopically light hydrothermal δ^{66}Zn signatures found amid the isotopically heavier abyssal ocean seawater (Conway and John, 2014a; John et al., 2018a; Lemaitre et al., 2020).

However, the persistent enrichments of dissolved Al, Fe, and Mn over thousands of kilometers of hydrothermal plume length was somewhat surprising for GEOTRACES oceanographers, because all three of these metals have sufficient oceanic scavenging rates to be otherwise net removed from hydrothermal plumes. Persistent hydrothermal dAl fluxes were explained at TAG by the tall rift valley walls that trap and concentrate dAl in the axial valley (Measures et al., 2015), and in the SEPR plume by a larger dAl source from the more actively erupting SEPR (Resing et al., 2015). Overall, it is thought that dAl has slow/negligible scavenging rates within hydrothermal plumes (Ho et al., 2019) due to dAl scavenging occurring predominantly by incorporation into siliceous particles that have low abundances in hydrothermal systems (Xu and Weber, 2021).

Dissolved Fe and Mn fluxes, speciation, and residence times within hydrothermal plumes have been a primary focus of the GEOTRACES program (Table 1). While early hydrothermal fluid research envisaged (near-)quantitative precipitation of hydrothermal Fe and Mn to the metalliferous sediments (German et al., 1991), similarities between dFe and ^{3}He profile shapes in far-field hydrothermal plumes (Fitzsimmons et al., 2014) introduced the possibility that only a fraction of the >10^{6}x enrichments in hydrothermal fluid Fe and Mn concentrations would need to be preserved in the dissolved phase to persist as a substantial enrichment in fully diluted hydrothermal plumes. This idea was called the "Leaky Vent Hypothesis" (Toner et al., 2012), and when an early global biogeochemical model of this "leaky" hydrothermal Fe flux tantalizingly hypothesized that hydrothermally sourced dFe could support a significant fraction of Southern Ocean export production (Tagliabue et al., 2010), interest in hydrothermal plume Fe fluxes skyrocketed. Subsequently, numerous early GEOTRACES studies confirmed the Leaky Vent Hypothesis (Klunder et al., 2011, 2012; Nishioka et al., 2013; Saito et al., 2013; Fitzsimmons et al., 2015; Hatta et al., 2015), providing global evidence for the persistence of dFe and dMn in hydrothermal plumes from the Arctic to the Southern Ocean and in every basin in between (Table 1). GEOTRACES then modified the research question from whether hydrothermal dFe and dMn persist in hydrothermal plumes to how and why they are protected from scavenging.

High-temperature hydrothermal vents supply Fe in its reduced oxidation state, Fe(II). Several GEOTRACES studies have investigated the contributions of Fe(II) to the hydrothermal plume dFe inventory and found them to vary substantially. Certain conditions can produce large hydrothermal Fe(II) enrichments, such as proximity to a fluid source (Sedwick et al., 2015; Holmes et al., 2020) and low oxygen and pH conditions that extend Fe(II) lifetimes. Otherwise, Fe(II) is rapidly oxidized to Fe(III) in most other hydrothermal plumes. González-Santana et al. (2021) have done important work within GEOTRACES to improve the parameterization of Fe(II) oxidation kinetics at temperatures more representative of the abyssal ocean conditions where hydrothermal plumes exist. This work revealed that the Fe(II) oxidation half-lives originally calculated for global hydrothermal plumes (Field and Sherrell, 2000) using original Fe(II) oxidation kinetics (Millero et al., 1987) were too short by about a factor of four, widening the area of plume influence within which Fe(II) is the dominant dFe species (Gartman and Findlay, 2020).

Because Fe(III) is minimally soluble in oxic seawater, what prevents hydrothermal Fe from quantitative precipitation and settling to the sediments? Two primary mechanisms have been proposed. The first proposes that Fe does in fact precipitate but only to nanoparticulate size, which still falls within the operationally defined dissolved size fraction. Nanoparticles do not sink to the sediments due to their small size, though imaging shows that Fe nanoparticles do aggregate into larger particles that settle to the sediments (Hoffman et al., 2020), perhaps facilitated by entrained organic carbon (Hoffman et al., 2018). While this nanoparticle mechanism was originally proposed for pyrite nanoparticles (Yucel et al., 2011), it has grown to include pervasive hydrothermal plume Fe oxyhydroxide nanoparticles as well, which have been implicated extensively in hydrothermal plume dFe transformations (Fitzsimmons et al., 2015, 2017; Lough et al., 2017, 2019a, 2019b, 2023; González-Santana et al., 2020).

The second mechanism proposes that hydrothermally sourced Fe is maintained in the dissolved phase via chelation by organic ligands, which effectively protect dFe against precipitation to the solid phase (Bennett et al., 2008; Sander and Koschinsky, 2011), similar to dCu as described above. Originally, electrochemical methods were used to analyze hydrothermal plume Fe-organic ligand complexes, including by both forward competitive ligand exchange mode (Bennett et al., 2008; Buck et al., 2015, 2018) and reverse titration mode (Hawkes et al., 2013). While valuable in indicating the lability of dFe complexes, electrochemical techniques unfortunately fail to differentiate nanoparticulate from ligand-bound dFe phases. Novel siderophore detection methods developed within GEOTRACES (e.g., Boiteau et al., 2016) and applied to hydrothermal plumes have revealed the presence of siderophores in a variety of plume settings from geotectonically distinct sites (Hoffman et al., 2023) that point to microbial origins (Cohen et al., 2021), perhaps as a way to access particulate Fe pools. While mechanistically interesting, siderophores only have sufficient concentrations to bind up to a few percent of total hydrothermal dFe.

In the absence of a fully diagnostic dFe physicochemical speciation method, Fe isotopic δ^{56}Fe analyses of hydrothermal

plume seawater have recently been used to relate Fe speciation in local cases (reviewed in Fitzsimmons and Conway, 2023). The large δ^{56}Fe fractionation during Fe(II)-Fe(III) reactions can be used to reveal the relative contributions of Fe(II) and Fe(III) in hydrothermal plumes (Klar et al., 2017). Additionally, under different conditions and assumptions, an isotopically heavy plume δ^{56}Fe signature has been employed to identify and/or quantify the persistence of organically chelated dFe species within distal hydrothermal plumes (Fitzsimmons et al., 2016, 2017; Sieber et al., 2021).

Finally, biogeochemical models calibrated against GEOTRACES datasets have been critical for probing metal speciation and scavenging rates and the biogeochemical fate of hydrothermal Fe. Hydrothermal Fe and Mn fluxes must be modeled with a significant gross hydrothermal fluid flux that is scavenged at high rates near the venting site in order to match the high dissolved metal gradients observed near ridge axes; for example, modeled hydrothermal Mn fluxes needed to be 96% scavenged near the vent outflow (van Hulten et al., 2017) to match observations in the North Atlantic.

For Fe, the potential for significant fertilization of Southern Ocean primary production and export by hydrothermal Fe (Ardyna et al., 2019) remains a major motivator for GEOTRACES studies of hydrothermal Fe plume dynamics. This is particularly true for Southern Ocean hydrothermal vents (Tagliabue and Resing, 2016), which would have the shortest transport timescale from abyssal plumes to surface phytoplankton. Unfortunately, the devil is in the details, and various models parameterize Fe speciation and transformations in slightly different ways, with these distinctions forming the difference between hydrothermal dFe being trapped in the deep ocean (Roshan et al., 2020) and efficient dFe fertilization of surface waters (Resing et al., 2015; Tagliabue et al., 2022). Additionally, none of the models include the shallow volcanoes and intraplate vents that have most recently been studied by GEOTRACES (German et al., 2020; Jenkins et al., 2020) and that can have large impacts on phytoplankton production (Guieu et al., 2018; Tilliette et al., 2022; Bonnet et al., 2023). Thus, even with its significant discoveries, GEOTRACES research has also stimulated many open questions for future observational and modeling research on the dynamics and biogeochemical impacts of hydrothermal plume Fe fluxes to answer.

CONCLUSIONS AND FUTURE WORK

We conclude with two primary messages. The first is that the elemental scavenging rates occurring in hydrothermal plumes are critical for quantifying the "net" hydrothermal impact on the ocean. The second is that research conducted within the international GEOTRACES program has significantly transformed our understanding of hydrothermal plume scavenging fluxes. We reviewed here the extensive GEOTRACES studies of hydrothermal plume geochemistry, and we sorted plume elemental behavior into five categories (Table 1, Figure 1) that represent a gradient in the extent of gross hydrothermal flux vs. scavenging that can be observed in hydrothermal systems.

In summary, while it was known as far back as Elderfield and Schultz (1996) that elements are removed from seawater in hydrothermal plumes, GEOTRACES studies have given us a mechanistic understanding of these plume scavenging processes, for example, providing partition coefficients (K_d) as a function of particle type (e.g., Fe oxyhydroxides, Mn oxides, organic carbon; Hayes et al., 2015b; Basak et al., 2024). These K_d values can be directly incorporated into biogeochemical models where particle types are designated (e.g., van Hulten et al., 2018). As a simple example of the impact of these calculations, globally interpolated hydrothermal plume scavenging fluxes onto Fe oxyhydroxides were projected to remove the equivalent of 5%–10% of the global riverine flux for Mo and twice the estimated riverine flux of V (Ho et al., 2018). GEOTRACES studies have also used radiotracer observations to quantify scavenging rates within hydrothermal plumes (Pavia et al., 2019). These rates can then be used directly in models themselves or used to ground-truth estimates of scavenging rates from prognostic models.

This new understanding of hydrothermal plume geochemical transformations has allowed us to imagine a future synthesis where the diverse fluxes of buoyant hydrothermal fluids can be combined with the potential scavenging fluxes within neutrally buoyant hydrothermal plumes to calculate the total "net" hydrothermal fluxes and impact on oceanic inventories across the globe. While the largest source of error was previously on the under-explored hydrothermal plume side, GEOTRACES has provided multiple pathways for calculating these scavenging rates. Arguably, today's largest source of error in calculating the "net" impact of hydrothermal plumes is in upscaling the variety of hydrothermal vent impacts to a global scale. These challenges include both extrapolating the gross hydrothermal fluid fluxes from different vent types (Diehl and Bach, 2020) to the global ocean, including the influence of the under-explored ultramafic and low-temperature diffuse-flow vents, and scaling up the spatiotemporal extent of scavenging within hydrothermal plumes of different vent types that contain different particle types and concentrations. Additionally, transformative research over the last two decades has, simultaneously with GEOTRACES, revealed the critical role that microbial activity plays in modifying chemical inventories within hydrothermal plumes (e.g. Dick et al., 2013; Cohen et al., 2021), providing a particularly rich opportunity for the geochemical and microbial oceanography communities to collaborate on distinguishing biotic from abiotic "scavenging" processes over the coming decade. Future hydrothermal plume research, born from the momentum of the GEOTRACES program, promises to deliver on these unknowns.

REFERENCES

Aguilar-Islas, A., H. Planquette, M.C. Lohan, W. Geibert, and G. Cutter. 2024. Intercalibration: A cornerstone of the success of the GEOTRACES program. *Oceanography* 37(2):21–24, https://doi.org/10.5670/oceanog.2024.404.

Alt, J.C. 2003. Hydrothermal fluxes at mid-ocean ridges and on ridge flanks. *Comptes Rendus Geoscience* 335(10):853–864, https://doi.org/10.1016/j.crte.2003.02.001.

Ardyna, M., L. Lacour, S. Sergi, F. d'Ovidio, J.-B. Sallée, M. Rembauville, S. Blain, A. Tagliabue, R. Schlitzer, C. Jeandel, and others. 2019. Hydrothermal vents trigger massive phytoplankton blooms in the Southern Ocean. *Nature Communications* 10(1):1–8, https://doi.org/10.1038/s41467-019-09973-6.

Basak, C., Y. Wu, B.A. Haley, J. Muratli, L.D. Pena, L. Bolge, J.N. Fitzsimmons, R.M. Sherrell, and S.L. Goldstein. 2024. Suspended particulate matter influence on dissolved Nd concentration and isotopic composition along GEOTRACES section GP16. *Earth and Planetary Science Letters* 635:118692, https://doi.org/10.1016/j.epsl.2024.118692.

Behrens, M.K., K. Pahnke, R. Paffrath, B. Schnetger, and H.-J. Brumsack. 2018. Rare earth element distributions in the West Pacific: Trace element sources and conservative vs. non-conservative behavior. *Earth and Planetary Science Letters* 486:166–177, https://doi.org/10.1016/j.epsl.2018.01.016.

Bemis, K., R.P. Lowell, and A. Farough. 2012. Diffuse flow: On and around hydrothermal vents at mid-ocean ridges. *Oceanography* 25(1):182–191, https://doi.org/10.5670/oceanog.2012.16.

Bennett, S.A., E.P. Achterberg, D.P. Connelly, P.J. Statham, G.R. Fones, and C.R. German. 2008. The distribution and stabilisation of dissolved Fe in deep-sea hydrothermal plumes. *Earth and Planetary Science Letters* 270:157–167, https://doi.org/10.1016/j.epsl.2008.01.048.

Bianchi, D., J.L. Sarmiento, A. Gnanadesikan, R.M. Key, P. Schlosser, and R. Newton. 2010. Low helium flux from the mantle inferred from simulations of oceanic helium isotope data. *Earth and Planetary Science Letters* 297(3–4):379–386, https://doi.org/10.1016/j.epsl.2010.06.037.

Boiteau, R.M., D.R. Mende, N.J. Hawco, M.R. McIlvin, J.N. Fitzsimmons, M.A. Saito, P.N. Sedwick, E.F. DeLong, and D.J. Repeta. 2016. Siderophore-based microbial adaptations to iron scarcity across the eastern Pacific Ocean. *Proceedings of the National Academy of Sciences of the United States of America* 113(50):14,237–14,242, https://doi.org/10.1073/pnas.1608594113.

Bonnet, S., C. Guieu, V. Taillandier, C. Boulart, P. Bouruet-Aubertot, F. Gazeau, C. Scalabrin, M. Bressac, A.N. Knapp, Y. Cuypers, and others. 2023. Natural iron fertilization by shallow hydrothermal sources fuels diazotroph blooms in the ocean. *Science* 380(6647):812–817, https://doi.org/10.1126/science.abq4654.

Boström, K., M.N.A. Peterson, O. Joensuu, and D.E. Fisher. 1969. Aluminum-poor ferromanganoan sediments on active oceanic ridges. *Journal of Geophysical Research* 74(12):3,261–3,270, https://doi.org/10.1029/JB074i012p03261.

Bowman, K.L., C.R. Hammerschmidt, C.H. Lamborg, and G. Swarr. 2015. Mercury in the North Atlantic Ocean: The U.S. GEOTRACES zonal and meridional sections. *Deep Sea Research Part II* 116:251–261, https://doi.org/10.1016/j.dsr2.2014.07.004.

Bowman, K.L., C.R. Hammerschmidt, C.H. Lamborg, G.J. Swarr, and A.M. Agather. 2016. Distribution of mercury species across a zonal section of the eastern tropical South Pacific Ocean (U.S. GEOTRACES GP16). *Marine Chemistry* 186:156–166, https://doi.org/10.1016/j.marchem.2016.09.005.

Boyle, E., S. Jiang, J.N. Fitzsimmons, and N.T. Lanning. 2020. Lead concentration and isotopic compositions in the central tropical Pacific Ocean. *Goldschmidt 2020 Abstract*, https://doi.org/10.46427/gold2020.244.

Bratkič, A., M. Vahčič, J. Kotnik, K. Obu Vazner, E. Begu, E.M.S. Woodward, and M. Horvat. 2016. Mercury presence and speciation in the South Atlantic Ocean along the 40°S transect. *Global Biogeochemical Cycles* 30(2):105–119, https://doi.org/10.1002/2015GB005275.

Brzezinski, M.A., and J.L. Jones. 2015. Coupling of the distribution of silicon isotopes to the meridional overturning circulation of the North Atlantic Ocean. *Deep Sea Research Part II* 116:79–88, https://doi.org/10.1016/j.dsr2.2014.11.015.

Buck, K.N., B. Sohst, and P.N. Sedwick. 2015. The organic complexation of dissolved iron along the U.S. GEOTRACES (GA03) North Atlantic Section. *Deep Sea Research Part II* 116:152–165, https://doi.org/10.1016/j.dsr2.2014.11.016.

Buck, K.N., P.N. Sedwick, B. Sohst, and C.A. Carlson. 2018. Organic complexation of iron in the eastern tropical South Pacific: Results from US GEOTRACES Eastern Pacific Zonal Transect (GEOTRACES cruise GP16). *Marine Chemistry* 201:229–241, https://doi.org/10.1016/j.marchem.2017.11.007.

Chan, C.-Y., L. Zheng, and Y. Sohrin. 2024. The behaviour of aluminium, manganese, iron, cobalt, and lead in the subarctic Pacific Ocean: Boundary scavenging and temporal changes. *Journal of Oceanography* 80(2):99–115, https://doi.org/10.1007/s10872-023-00710-8.

Charette, M.A., P.J. Morris, P.B. Henderson, and W.S. Moore. 2015. Radium isotope distributions during the US GEOTRACES North Atlantic cruises. *Marine Chemistry* 177(Part 1):184–195, https://doi.org/10.1016/j.marchem.2015.01.001.

Charlou, J.L., J.P. Donval, C. Konn, H. Ondréas, Y. Fouquet, P. Jean-Baptiste, and E. Fourré. 2010. High production and fluxes of H_2 and CH_4 and evidence of abiotic hydrocarbon synthesis by serpentinization in ultramafic-hosted hydrothermal systems on the Mid-Atlantic Ridge. Pp. 265–296 in *Diversity of Hydrothermal Systems on Slow Spreading Ocean Ridges.* P.A. Rona, C.W. Devey, J. Dyment, and B.J. Murton, eds, https://doi.org/10.1029/2008GM000752.

Chinni, V., S.K. Singh, R. Bhushan, R. Rengarajan, and V.V.S.S. Sarma. 2019. Spatial variability in dissolved iron concentrations in the marginal and open waters of the Indian Ocean. *Marine Chemistry* 208:11–28, https://doi.org/10.1016/j.marchem.2018.11.007.

Chinni, V., and S.K. Singh. 2022. Dissolved iron cycling in the Arabian Sea and sub-tropical gyre region of the Indian Ocean. *Geochimica et Cosmochimica Acta* 317:325–348, https://doi.org/10.1016/j.gca.2021.10.026.

Chmiel, R., N. Lanning, A. Laubach, J.M. Lee, J. Fitzsimmons, M. Hatta, W. Jenkins, P. Lam, M. McIlvin, A. Tagliabue, and others. 2022. Major processes of the dissolved cobalt cycle in the North and equatorial Pacific Ocean. *Biogeosciences* 19(9):2,365–2,395, https://doi.org/10.5194/bg-19-2365-2022.

Cohen, N.R., A.E. Noble, D.M. Moran, M.R. McIlvin, T.J. Goepfert, N.J. Hawco, C.R. German, T.J. Horner, C.H. Lamborg, J.P. McCrow, and others. 2021. Hydrothermal trace metal release and microbial metabolism in the northeastern Lau Basin of the South Pacific Ocean. *Biogeosciences* 18(19):5,397–5,422, https://doi.org/10.5194/bg-18-5397-2021.

Conway, T.M., and S.G. John. 2014a. The biogeochemical cycling of zinc and zinc isotopes in the North Atlantic Ocean. *Global Biogeochemical Cycles* 28(10):1,111–1,128, https://doi.org/10.1002/2014GB004862.

Conway, T.M., and S.G. John. 2014b. Quantification of dissolved iron sources to the North Atlantic Ocean. *Nature* 511(7508):212–215, https://doi.org/10.1038/nature13482.

Conway, T.M., and S.G. John. 2015. Biogeochemical cycling of cadmium isotopes along a high-resolution section through the North Atlantic Ocean. *Geochimica et Cosmochimica Acta* 148:269–283, https://doi.org/10.1016/j.gca.2014.09.032.

Conway, T.M., R. Middag, and R. Schlitzer. 2024. GEOTRACES: Ironing out the details of the oceanic iron sources? *Oceanography* 37(2):35–45, https://doi.org/10.5670/oceanog.2024.416.

Corliss, J.B., M. Lyle, J. Dymond, and K. Crane. 1978. The chemistry of hydrothermal mounds near the Galapagos Rift. *Earth and Planetary Science Letters* 40(1):12–24, https://doi.org/10.1016/0012-821X(78)90070-5.

Dick, G., K. Anantharaman, B. Baker, M. Li, D. Reed, and C. Sheik. 2013. The microbiology of deep-sea hydrothermal vent plumes: Ecological and biogeographic linkages to seafloor and water column habitats. *Frontiers in Microbiology* 4:124, https://doi.org/10.3389/fmicb.2013.00124.

Diehl, A., and W. Bach. 2020. MARHYS (MARine HYdrothermal Solutions) database: A global compilation of marine hydrothermal vent fluid, end member, and seawater compositions. *Geochemistry, Geophysics, Geosystems* 21(12):e2020GC009385, https://doi.org/10.1029/2020GC009385.

Edmond, J.M., C. Measures, R. McDuff, L. Chan, R. Collier, B. Grant, L. Gordon, and J. Corliss. 1979. Ridge crest hydrothermal activity and the balances of the major and minor elements in the ocean: The Galapagos data. *Earth and Planetary Science Letters* 46(1):1–18, https://doi.org/10.1016/0012-821X(79)90061-X.

Edmond, J.M., K.L. Von Damm, R.E. McDuff, and C.I. Measures. 1982. Chemistry of hot springs on the East Pacific Rise and their effluent dispersal. *Nature* 297(5863):187–191, https://doi.org/10.1038/297187a0.

Elderfield, H., and A. Schultz. 1996. Mid-ocean ridge hydrothermal fluxes and the chemical composition of the ocean. *Earth and Planetary Science Letters* 24:191–224, https://doi.org/10.1146/annurev.earth.24.1.191.

Feely, R.A., G.J. Massoth, E.T. Baker, J.P. Cowen, M.F. Lamb, and K.A. Krogslund. 1990. The effect of hydrothermal processes on midwater phosphorus distributions in the northeast Pacific. *Earth and Planetary Science Letters* 96(3):305–318, https://doi.org/10.1016/0012-821X(90)90009-M.

Field, M.P., and R.M. Sherrell. 2000. Dissolved and particulate Fe in a hydrothermal plume at 9°45'N, East Pacific Rise: Slow Fe(II) oxidation kinetics in Pacific plumes. *Geochimica Et Cosmochimica Acta* 64(4):619–628, https://doi.org/10.1016/S0016-7037(99)00333-6.

Fitzsimmons, J.N., W.J. Jenkins, and E.A. Boyle. 2014. Distal transport of dissolved hydrothermal iron in the deep South Pacific Ocean. *Proceedings of the National Academy of Sciences of the United States of America* 111(47):16,654–16,661, https://doi.org/10.1073/pnas.1418778hy111.

Fitzsimmons, J.N., G.G. Carrasco, J. Wu, S. Roshan, M. Hatta, C.I. Measures, T.M. Conway, S.G. John, and E.A. Boyle. 2015. Partitioning of dissolved iron and iron isotopes into soluble and colloidal phases along the GA03 GEOTRACES North Atlantic Transect. *Deep Sea Research II* 116:130–151, https://doi.org/10.1016/j.dsr2.2014.11.014.

Fitzsimmons, J.N., T.M. Conway, J.-M. Lee, R. Kayser, K.M. Thyng, S.G. John, and E.A. Boyle. 2016. Dissolved iron and iron isotopes in the Southeastern Pacific Ocean. *Global Biogeochemical Cycles* 30(10):1,372–1,395, https://doi.org/10.1002/2015GB005357.

Fitzsimmons, J.N., S.G. John, C.M. Marsay, C.L. Hoffman, S.L. Nicholas, B.M. Toner, C.R. German, and R.M. Sherrell. 2017. Iron persistence in a distal hydrothermal plume supported by dissolved-particulate exchange. *Nature Geoscience* 10:195–201, https://doi.org/10.1038/ngeo2900.

Fitzsimmons, J.N., and T.M. Conway. 2023. Novel insights into marine iron biogeochemistry from iron isotopes. *Annual Review of Marine Science* 15(1):383–406, https://doi.org/10.1146/annurev-marine-032822-103431.

Gamo, T., K. Okamura, H. Hatanaka, H. Hasumoto, D. Komatsu, M. Chinen, M. Mori, J. Tanaka, A. Hirota, U. Tsunogai, and others. 2015. Hydrothermal plumes in the Gulf of Aden, as characterized by light transmission, Mn, Fe, CH_4 and $\delta^{13}C–CH_4$ anomalies. *Deep Sea Research Part II* 121:62–70, https://doi.org/10.1016/j.dsr2.2015.06.004.

Gartman, A., and A.J. Findlay. 2020. Impacts of hydrothermal plume processes on oceanic metal cycles and transport. *Nature Geoscience* 13(6):396–402, https://doi.org/10.1038/s41561-020-0579-0.

Gdaniec, S., M. Roy-Barman, M. Levier, O. Valk, M.R. van der Loeff, L. Foliot, A. Dapoigny, L. Missiaen, C.-M. Mörth, and P.S. Andersson. 2020. ^{231}Pa and ^{230}Th in the Arctic Ocean: Implications for boundary scavenging and $^{231}Pa–^{230}Th$ fractionation in the Eurasian Basin. *Chemical Geology* 532:119380, https://doi.org/10.1016/j.chemgeo.2019.119380.

GEOTRACES Planning Group. 2006. *GEOTRACES Science Plan*. Scientific Committee on Oceanic Research, Baltimore, MD, https://geotracesold.sedoo.fr/libraries/documents/Science_plan.pdf.

German, C.R., A.C. Campbell, and J.M. Edmond. 1991. Hydrothermal scavenging at the Mid-Atlantic Ridge: Modification of trace element dissolved fluxes. *Earth and Planetary Science Letters* 107(1):101–114, https://doi.org/10.1016/0012-821X(91)90047-L.

German, C.R., J.A. Resing, G. Xu, I.A. Yeo, S.L. Walker, C.W. Devey, J.W. Moffett, G.A. Cutter, O. Hyvernaud, and D. Reymond. 2020. Hydrothermal activity and seismicity at Teahitia Seamount: Reactivation of the Society Islands hotspot? *Frontiers in Marine Science* 7:73, https://doi.org/10.3389/fmars.2020.00073.

German, C.R., S.Q. Lang, and J.N. Fitzsimmons. In press. Hydrothermal processes. In *Treatise on Geochemistry*. A.D. Anbar, and D. Weis, eds.

Gerringa, L.J.A., M.J.A. Rijkenberg, H.A. Slagter, P. Laan, R. Paffrath, D. Bauch, M. Rutgers van der Loeff, and R. Middag. 2021. Dissolved Cd, Co, Cu, Fe, Mn, Ni, and Zn in the Arctic Ocean. *Journal of Geophysical Research: Oceans* 126(9), https://doi.org/10.1029/2021JC017323.

González-Santana, D., H. Planquette, M. Cheize, H. Whitby, A. Gourain, T. Holmes, V. Guyader, C. Cathalot, E. Pelleter, Y. Fouquet, and others. 2020. Processes driving iron and manganese dispersal from the TAG hydrothermal plume (Mid-Atlantic Ridge): Results from a GEOTRACES process study. *Frontiers in Marine Science* 7, https://doi.org/10.3389/fmars.2020.00568.

González-Santana, D., M. González-Dávila, M.C. Lohan, L. Artigue, H. Planquette, G. Sarthou, A. Tagliabue, and J.M. Santana-Casiano. 2021. Variability in iron (II) oxidation kinetics across diverse hydrothermal sites on the northern Mid Atlantic Ridge. *Geochimica et Cosmochimica Acta* 297:143–157, https://doi.org/10.1016/j.gca.2021.01.013.

Grasse, P., I. Closset, J.L. Jones, S. Geilert, and M.A. Brzezinski. 2020. Controls on dissolved silicon isotopes along the US GEOTRACES Eastern Pacific Zonal Transect (GP16). *Global Biogeochemical Cycles* 34(9):e2020GB006538, https://doi.org/10.1029/2020GB006538.

Guieu, C., S. Bonnet, A. Petrenko, C. Menkes, V. Chavagnac, K. Desboeufs, C. Maes, and T. Moutin. 2018. Iron from a submarine source impacts the productive layer of the western tropical South Pacific (WTSP). *Scientific Reports* 8(1):9075, https://doi.org/10.1038/s41598-018-27407-z.

Hatta, M., C.I. Measures, S. Roshan, J. Wu, J.N. Fitzsimmons, P. Sedwick, and P.L. Morton. 2015. An overview of dissolved Fe and Mn distributions during the 2010–2011 US GEOTRACES North Atlantic cruises: GEOTRACES GA03. *Deep Sea Research Part II* 116:117–129, https://doi.org/10.1016/j.dsr2.2014.07.005.

Hawco, N.J., D.C. Ohnemus, J.A. Resing, B.S. Twining, and M.A. Saito. 2016. A dissolved cobalt plume in the oxygen minimum zone of the eastern tropical South Pacific. *Biogeosciences* 13(20):5,697–5,717, https://doi.org/10.5194/bg-13-5697-2016.

Hawkes, J.A., D.P. Connelly, M. Gledhill, and E.P. Achterberg. 2013. The stabilisation and transportation of dissolved iron from high temperature hydrothermal vent systems. *Earth and Planetary Science Letters* 375(0):280–290, https://doi.org/10.1016/j.epsl.2013.05.047.

Hayes, C.T., R.F. Anderson, M.Q. Fleisher, K.-F. Huang, L.F. Robinson, Y. Lu, H. Cheng, R.L. Edwards, and S.B. Moran. 2015a. ^{230}Th and ^{231}Pa on GEOTRACES GA03, the US GEOTRACES North Atlantic transect, and implications for modern and paleoceanographic chemical fluxes. *Deep Sea Research Part II* 116:29–41, https://doi.org/10.1016/j.dsr2.2014.07.007.

Hayes, C.T., R.F. Anderson, M.Q. Fleisher, S.M. Vivancos, P.J. Lam, D.C. Ohnemus, K.-F. Huang, L.F. Robinson, Y. Lu, H. Cheng, and others. 2015b. Intensity of Th and Pa scavenging partitioned by particle chemistry in the North Atlantic Ocean. *Marine Chemistry* 170:49–60, https://doi.org/10.1016/j.marchem.2015.01.006.

Ho, P., J.-M. Lee, M.I. Heller, P.J. Lam, and A.M. Shiller. 2018. The distribution of dissolved and particulate Mo and V along the US GEOTRACES East Pacific Zonal Transect (GP16): The roles of oxides and biogenic particles in their distributions in the oxygen deficient zone and the hydrothermal plume. *Marine Chemistry* 201:242–255, https://doi.org/10.1016/j.marchem.2017.12.003.

Ho, P., J.A. Resing, and A.M. Shiller. 2019. Processes controlling the distribution of dissolved Al and Ga along the US GEOTRACES East Pacific Zonal Transect (GP16). *Deep Sea Research Part I* 147:128–145, https://doi.org/10.1016/j.dsr.2019.04.009.

Hoffman, C.L., S.L. Nicholas, D.C. Ohnemus, J.N. Fitzsimmons, R.M. Sherrell, C.R. German, M.I. Heller, J.-m. Lee, P.J. Lam, and B.M. Toner. 2018. Near-field iron and carbon chemistry of non-buoyant hydrothermal plume particles, Southern East Pacific Rise 15°S. *Marine Chemistry* 201:183–197, https://doi.org/10.1016/j.marchem.2018.01.011.

Hoffman, C.L., C.S. Schladweiler, N.C.A. Seaton, S.L. Nicholas, J.N. Fitzsimmons, R.M. Sherrell, C.R. German, P.J. Lam, and B.M. Toner. 2020. Diagnostic morphology and solid-state chemical speciation of hydrothermally derived particulate Fe in a long-range dispersing plume. *ACS Earth and Space Chemistry* 4(10):1,831–1,842, https://doi.org/10.1021/acsearthspacechem.0c00067.

Hoffman, C.L., P.J. Monreal, J.B. Albers, A.J.M. Lough, A.E. Santoro, T. Mellett, K.N. Buck, A. Tagliabue, M.C. Lohan, J.A. Resing, and others. 2023. Microbial strong organic ligand production is tightly coupled to iron in hydrothermal plumes. bioRxiv preprint, https://doi.org/10.1101/2023.01.05.522639.

Holmes, T.M., K. Wuttig, Z. Chase, C. Schallenberg, P. van der Merwe, A.T. Townsend, and A.R. Bowie. 2020. Glacial and hydrothermal sources of dissolved iron (II) in Southern Ocean waters surrounding Heard and McDonald Islands. *Journal of Geophysical Research: Oceans* 125(10):e2020JC016286, https://doi.org/10.1029/2020JC016286.

Humphris, S.E., and G. Thompson. 1978. Hydrothermal alteration of oceanic basalts by seawater. *Geochimica et Cosmochimica Acta* 42(1):107–125, https://doi.org/10.1016/0016-7037(78)90221-1.

Jacquot, J.E., and J.W. Moffett. 2015. Copper distribution and speciation across the International GEOTRACES Section GA03. *Deep Sea Research Part II* 116:187–207, https://doi.org/10.1016/j.dsr2.2014.11.013.

Janssen, D.J., D. Gilliard, J. Rickli, P. Nasemann, A. Koschinsky, C.S. Hassler, A.R. Bowie, M.J. Ellwood, C. Kleint, and S.L. Jaccard. 2023. Chromium stable isotope distributions in the southwest Pacific Ocean and constraints on hydrothermal input from the Kermadec Arc. *Geochimica et Cosmochimica Acta* 342:31–44, https://doi.org/10.1016/j.gca.2022.12.010.

Jenkins, W.J., D.E. Lott, B.E. Longworth, J.M. Curtice, and K.L. Cahill. 2015. The distributions of helium isotopes and tritium along the US GEOTRACES North Atlantic sections (GEOTRACES GAO3). *Deep Sea Research Part II* 116:21–28, https://doi.org/10.1016/j.dsr2.2014.11.017.

Jenkins, W.J., D.E. Lott, C.R. German, K.L. Cahill, J. Goudreau, and B. Longworth. 2018. The deep distributions of helium isotopes, radiocarbon, and noble gases along the US GEOTRACES East Pacific Zonal Transect (GP16). *Marine Chemistry* 201:167–182, https://doi.org/10.1016/j.marchem.2017.03.009.

Jenkins, W.J., S.C. Doney, M. Fendrock, R. Fine, T. Gamo, P. Jean-Baptiste, R. Key, B. Klein, J.E. Lupton, R. Newton, and others. 2019. A comprehensive global oceanic dataset of helium isotope and tritium measurements. *Earth System Science Data* 11(2):441–454, https://doi.org/10.5194/essd-11-441-2019.

Jenkins, W.J., M. Hatta, J.N. Fitzsimmons, R. Schlitzer, N.T. Lanning, A. Shiller, N.R. Buckley, C.R. German, D.E. Lott, G. Weiss, and others. 2020. An intermediate-depth source of hydrothermal ^{3}He and dissolved iron in the North Pacific. *Earth and Planetary Science Letters* 539:116223, https://doi.org/10.1016/j.epsl.2020.116223.

Jenkins, W.J., S.C. Doney, A.M. Seltzer, C.R. German, D.E. Lott, and K.L. Cahill. 2023. A North Pacific meridional section (US GEOTRACES GP15) of helium isotopes and noble gases: Part I. Deep water distributions. *Global Biogeochemical Cycles* 37(5), 10.1029/2022gb007667, https://doi.org/10.1029/2022GB007667.

John, S.G., and T.M. Conway. 2014. A role for scavenging in the marine biogeochemical cycling of zinc and zinc isotopes. *Earth and Planetary Science Letters* 394:159–167, https://doi.org/10.1016/j.epsl.2014.02.053.

John, S.G., J. Helgoe, and E. Townsend. 2018a. Biogeochemical cycling of Zn and Cd and their stable isotopes in the Eastern Tropical South Pacific. *Marine Chemistry* 201:256–262, https://doi.org/10.1016/j.marchem.2017.06.001.

John, S.G., J. Helgoe, E. Townsend, T. Weber, T. DeVries, A. Tagliabue, K. Moore, P. Lam, C.M. Marsay, and C. Till. 2018b. Biogeochemical cycling of Fe and Fe stable isotopes in the Eastern Tropical South Pacific. *Marine Chemistry* 201:66–76, https://doi.org/10.1016/j.marchem.2017.06.003.

Kadko, D., J. Baross, and J. Alt. 1995. The magnitude and global implications of hydrothermal flux. *Geophysical Monograph-American Geophysical Union* 91:Pp. 446–446 in *Seafloor Hydrothermal Systems: Physical, Chemical, Biological, and Geological Interactions*. Geophysical Monograph Series, vol. 91, S.E. Humphris, R.A. Zirenberg, L.S. Mullineaux, and R.E. Thomson, eds, American Geophysical Union, Washington, DC, https://doi.org/10.1029/GM091p0446.

Kelley, D.S., J.A. Karson, G.L. Fruh-Green, D.R. Yoerger, T.M. Shank, D.A. Butterfield, J.M. Hayes, M.O. Schrenk, E.J. Olson, G. Proskurowski, and others. 2005. A serpentinite-hosted ecosystem: The Lost City hydrothermal field. *Science* 307(5714):1,428–1,434, https://doi.org/10.1126/science.1102556.

Kipp, L.E., M.A. Charette, D.E. Hammond, and W.S. Moore. 2015. Hydrothermal vents: A previously unrecognized source of actinium-227 to the deep ocean. *Marine Chemistry* 177:583–590, https://doi.org/10.1016/j.marchem.2015.09.002.

Kipp, L.E., V. Sanial, P.B. Henderson, P. van Beek, J.-L. Reyss, D.E. Hammond, W.S. Moore, and M.A. Charette. 2018. Radium isotopes as tracers of hydrothermal inputs and neutrally buoyant plume dynamics in the deep ocean. *Marine Chemistry* 201:51–65, https://doi.org/10.1016/j.marchem.2017.06.011.

Klar, J.K., R.H. James, D. Gibbs, A. Lough, I. Parkinson, J.A. Milton, J.A. Hawkes, and D.P. Connelly. 2017. Isotopic signature of dissolved iron delivered to the Southern Ocean from hydrothermal vents in the East Scotia Sea. *Geology* 45(4):351–354, https://doi.org/10.1130/G38432.1.

Klunder, M.B., P. Laan, R. Middag, H.J.W. De Baar, and J.C. van Ooijen. 2011. Dissolved iron in the Southern Ocean (Atlantic sector). *Deep Sea Research Part II* 58(25–26):2,678–2,694, https://doi.org/10.1016/j.dsr2.2010.10.042.

Klunder, M.B., P. Laan, R. Middag, H.J.W. de Baar, and K. Bakker. 2012. Dissolved iron in the Arctic Ocean: Important role of hydrothermal sources, shelf input and scavenging removal. *Journal of Geophysical Research: Oceans* 117(C4), https://doi.org/10.1029/2011JC007135.

Le Roy, E., V. Sanial, M.A. Charette, P. van Beek, F. Lacan, S.H.M. Jacquet, P.B. Henderson, M. Souhaut, M.I. García-Ibáñez, C. Jeandel, and others. 2018. The ^{226}Ra-Ba relationship in the North Atlantic during GEOTRACES-GA01. *Biogeosciences* 15(9):3,027–3,048, https://doi.org/10.5194/bg-15-3027-2018.

Le Roy, E., P. Van Beek, F. Lacan, M. Souhaut, V. Sanial, M.A. Charette, P.B. Henderson, and F. Deng. 2023. The distribution of ^{227}Ac along the GA01 section in the North Atlantic. *Marine Chemistry* 248:104207, https://doi.org/10.1016/j.marchem.2023.104207.

Lee, J.-M., M.I. Heller, and P.J. Lam. 2018. Size distribution of particulate trace elements in the US GEOTRACES Eastern Pacific Zonal Transect (GP16). *Marine Chemistry* 201:108–123, https://doi.org/10.1016/j.marchem.2017.09.006.

Lemaitre, N., G.F. de Souza, C. Archer, R.-M. Wang, H. Planquette, G. Sarthou, and D. Vance. 2020. Pervasive sources of isotopically light zinc in the North Atlantic Ocean. *Earth and Planetary Science Letters* 539:116216, https://doi.org/10.1016/j.epsl.2020.116216.

Liguori, B.T., C. Ehlert, and K. Pahnke. 2020. The influence of water mass mixing and particle dissolution on the silicon cycle in the central Arctic Ocean. *Frontiers in Marine Science* 7:202, https://doi.org/10.3389/fmars.2020.00202.

Lilley, M.D., R.A. Feely, and J.H. Trefry. 1995. Chemical and biochemical transformations in hydrothermal plumes. Pp. 369–391 in *Seafloor Hydrothermal Systems: Physical, Chemical, Biological, and Geological Interactions.* Geophysical Monograph Series, vol. 91, S.E. Humphris, R.A. Zirenberg, L.S. Mullineaux, and R.E. Thomson, eds, American Geophysical Union, Washington, DC, https://doi.org/10.1029/GM091p0369.

Little, S.H., C. Archer, A. Milne, C. Schlosser, E.P. Achterberg, M.C. Lohan, and D. Vance. 2018. Paired dissolved and particulate phase Cu isotope distributions in the South Atlantic. *Chemical Geology* 502:29–43, https://doi.org/10.1016/j.chemgeo.2018.07.022.

Lough, A., J. Klar, W. Homoky, S. Comer-Warner, J. Milton, D. Connelly, R. James, and R. Mills. 2017. Opposing authigenic controls on the isotopic signature of dissolved iron in hydrothermal plumes. *Geochimica et Cosmochimica Acta* 202:1–20, https://doi.org/10.1016/j.gca.2016.12.022.

Lough, A.J.M., D.P. Connelly, W.B. Homoky, J.A. Hawkes, V. Chavagnac, A. Castillo, M. Kazemian, K.-i. Nakamura, T. Araki, B. Kaulich, and others. 2019a. Diffuse hydrothermal venting: A hidden source of iron to the oceans. *Frontiers in Marine Science* 6:329, https://doi.org/10.3389/fmars.2019.00329.

Lough, A.J.M., W.B. Homoky, D.P. Connelly, S.A. Comer-Warner, K. Nakamura, M.K. Abyaneh, B. Kaulich, and R.A. Mills. 2019b. Soluble iron conservation and colloidal iron dynamics in a hydrothermal plume. *Chemical Geology* 511:225–237, https://doi.org/10.1016/j.chemgeo.2019.01.001.

Lough, A.J.M., A. Tagliabue, C. Demasy, J.A. Resing, T. Mellett, N.J. Wyatt, and M.C. Lohan. 2023. Tracing differences in iron supply to the Mid-Atlantic Ridge valley between hydrothermal vent sites: Implications for the addition of iron to the deep ocean. *Biogeosciences* 20(2):405–420, https://doi.org/10.5194/bg-20-405-2023.

Lupton, J.E., and H. Craig. 1981. A major helium-3 source at 15°S on the East Pacific Rise. *Science* 214(4516):13–18, https://doi.org/10.1126/science.214.4516.13.

Lupton, J.E. 1995. Hydrothermal plumes: Near and far field. Pp. 317–346, in *Seafloor Hydrothermal Systems: Physical, Chemical, Biological, and Geological Interactions*. Geophysical Monograph Series, vol. 91, S.E. Humphris, R.A. Zirenberg, L.S. Mullineaux, and R.E. Thomson, eds, American Geophysical Union, Washington, DC, https://doi.org/10.1029/GM091p0317.

Lupton, J.E., and W.J. Jenkins. 2017. Evolution of the South Pacific helium plume over the past three decades. *Geochemistry, Geophysics, Geosystems* 18(5):1,810–1,823, https://doi.org/10.1002/2017GC006848.

Mackenzie, F.T., and R.M. Garrels. 1966. Chemical mass balance between rivers and oceans. *American Journal of Science* 264(7):507–525, https://doi.org/10.2475/ajs.264.7.507.

Measures, C.I., M. Hatta, J.N. Fitzsimmons, and P.L. Morton. 2015. Dissolved Al in the zonal N Atlantic section of the US GETORACES 2010/2011 cruises and the importance of hydrothermal inputs. *Deep Sea Research Part II* 116:176–186, https://doi.org/10.1016/j.dsr2.2014.07.006.

Measures, C., and M. Hatta. 2021. On using Si to unravel potential sources of dissolved Al to the deep Arctic. *Journal of Geophysical Research: Oceans* 126(10), https://doi.org/10.1029/2021JC017399.

Middag, R., H.J.W. De Baar, P. Laan, and K. Bakker. 2009. Dissolved aluminium and the silicon cycle in the Arctic Ocean. *Marine Chemistry* 115(3–4):176–195, https://doi.org/10.1016/j.marchem.2009.08.002.

Middag, R., M.M.P. van Hulten, H.M. Van Aken, M.J.A. Rijkenberg, L.J.A. Gerringa, P. Laan, and H.J.W. de Baar. 2015. Dissolved aluminium in the ocean conveyor of the West Atlantic Ocean: Effects of the biological cycle, scavenging, sediment resuspension and hydrography. *Marine Chemistry* 177:69–86, https://doi.org/10.1016/j.marchem.2015.02.015.

Millero, F.J., S. Sotolongo, and M. Izaguirre. 1987. The oxidation kinetics of Fe(II) in seawater. *Geochimica et Cosmochimica Acta* 51:793–801, https://doi.org/10.1016/0016-7037(87)90093-7.

Moffett, J.W., and J. Ho. 1996. Oxidation of cobalt and manganese in seawater via a common microbially catalyzed pathway. *Geochimica et Cosmochimica Acta* 60(18):3,415–3,424, https://doi.org/10.1016/0016-7037(96)00176-7.

Mottl, M.J., and T.F. McConachy. 1990. Chemical processes in buoyant hydrothermal plumes on the East Pacific Rise near 21°N. *Geochimica et Cosmochimica Acta* 54(7):1,911–1,927, https://doi.org/10.1016/0016-7037(90)90261-I.

Neuholz, R., C. Kleint, B. Schnetger, A. Koschinsky, P. Laan, R. Middag, S. Sander, J. Thal, A. Türke, M. Walter, and others. 2020a. Submarine hydrothermal discharge and fluxes of dissolved Fe and Mn, and He isotopes at Brothers Volcano based on radium isotopes. *Minerals* 10(11), https://doi.org/10.3390/min10110969.

Neuholz, R., B. Schnetger, C. Kleint, A. Koschinsky, K. Lettmann, S. Sander, A. Türke, M. Walter, R. Zitoun, and H.-J. Brumsack. 2020b. Near-field hydrothermal plume dynamics at Brothers Volcano (Kermadec Arc): A short-lived radium isotope study. *Chemical Geology* 533:119379, https://doi.org/10.1016/j.chemgeo.2019.119379.

Niedermiller, J., and M. Baskaran. 2019. Comparison of the scavenging intensity, remineralization and residence time of ^{210}Po and ^{210}Pb at key zones (biotic, sediment-water and hydrothermal) along the East Pacific GEOTRACES transect. *Journal of Environmental Radioactivity* 198:165–188, https://doi.org/10.1016/j.jenvrad.2018.12.016.

Nishioka, J., H. Obata, and D. Tsumune. 2013. Evidence of an extensive spread of hydrothermal dissolved iron in the Indian Ocean. *Earth and Planetary Science Letters* 361:26–33, https://doi.org/10.1016/j.epsl.2012.11.040.

Noble, A.E., Y. Echegoyen-Sanz, E.A. Boyle, D.C. Ohnemus, P.J. Lam, R. Kayser, M. Reuer, J. Wu, and W. Smethie. 2015. Dynamic variability of dissolved Pb and Pb isotope composition from the US North Atlantic GEOTRACES transect. *Deep Sea Research Part II* 116:208–225, https://doi.org/10.1016/j.dsr2.2014.11.011.

Noble, A.E., D.C. Ohnemus, N.J. Hawco, P.J. Lam, and M.A. Saito. 2017. Coastal sources, sinks and strong organic complexation of dissolved cobalt within the US North Atlantic GEOTRACES transect GA03. *Biogeosciences* 14(11):2,715–2,739, https://doi.org/10.5194/bg-14-2715-2017.

Paffrath, R., K. Pahnke, P. Böning, M. Rutgers van der Loeff, O. Valk, S. Gdaniec, and H. Planquette. 2021. Seawater-particle interactions of rare earth elements and neodymium isotopes in the deep central Arctic Ocean. *Journal of Geophysical Research: Oceans* 126(8):e2021JC017423, https://doi.org/10.1029/2021JC017423.

Pagnone, A., C. Völker, and Y. Ye. 2019. Processes affecting dissolved iron across the Subtropical North Atlantic: A model study. *Ocean Dynamics* 69(9):989–1,007, https://doi.org/10.1007/s10236-019-01288-w.

Pavia, F., R.F. Anderson, S.M. Vivancos, M.Q. Fleisher, P.J. Lam, Y. Lu, H. Cheng, P. Zhang, and R.L. Edwards. 2018. Intense hydrothermal scavenging of ^{230}Th and ^{231}Pa in the deep Southeast Pacific. *Marine Chemistry* 201:212–228, https://doi.org/10.1016/j.marchem.2017.08.003.

Pavia, F.J., R.F. Anderson, E.E. Black, L.E. Kipp, S.M. Vivancos, M.Q. Fleisher, M.A. Charette, V. Sanial, W.S. Moore, M. Hult, and others. 2019. Timescales of hydrothermal scavenging in the South Pacific Ocean from ^{234}Th, ^{230}Th, and ^{228}Th. *Earth and Planetary Science Letters* 506:146–156, https://doi.org/10.1016/j.epsl.2018.10.038.

Rahman, S., A.M. Shiller, R.F. Anderson, M.A. Charette, C.T. Hayes, M. Gilbert, K.R. Grissom, P.J. Lam, D.C. Ohnemus, F.J. Pavia, and others. 2022. Dissolved and particulate barium distributions along the US GEOTRACES North Atlantic and East Pacific zonal transects (GA03 and GP16): Global implications for the marine barium cycle. *Global Biogeochemical Cycles* 36(6):e2022GB007330, https://doi.org/10.1029/2022GB007330.

Resing, J.A., P.N. Sedwick, C.R. German, W.J. Jenkins, J.W. Moffett, B.M. Sohst, and A. Tagliabue. 2015. Basin-scale transport of hydrothermal dissolved metals across the South Pacific Ocean. *Nature* 523:200–206, https://doi.org/10.1038/nature14577.

Rigaud, S., G. Stewart, M. Baskaran, D. Marsan, and T. Church. 2015. ^{210}Po and ^{210}Pb distribution, dissolved-particulate exchange rates, and particulate export along the North Atlantic US GEOTRACES GA03 section. *Deep Sea Research Part II* 116:60–78, https://doi.org/10.1016/j.dsr2.2014.11.003.

Rijkenberg, M.J., R. Middag, P. Laan, L.J.A. Gerringa, H.M. van Aken, V. Schoemann, J.T. de Jong, and H.J.W. de Baar. 2014. The distribution of dissolved iron in the West Atlantic Ocean. *PLoS One* 9(6):e101323, https://doi.org/10.1371/journal.pone.0101323.

Roshan, S., and J. Wu. 2015a. The distribution of dissolved copper in the tropical-subtropical north Atlantic across the GEOTRACES GA03 transect. *Marine Chemistry* 176:189–198, https://doi.org/10.1016/j.marchem.2015.09.006.
Roshan, S., and J. Wu. 2015b. Water mass mixing: The dominant control on the zinc distribution in the North Atlantic Ocean. *Global Biogeochemical Cycles* 29(7):1,060–1,074, https://doi.org/10.1002/2014GB005026.
Roshan, S., J. Wu, and W.J. Jenkins. 2016. Long-range transport of hydrothermal dissolved Zn in the tropical South Pacific. *Marine Chemistry* 183:25–32, https://doi.org/10.1016/j.marchem.2016.05.005.
Roshan, S., and J. Wu. 2018. Dissolved and colloidal copper in the tropical South Pacific. *Geochimica et Cosmochimica Acta* 233:81–94, https://doi.org/10.1016/j.gca.2018.05.008.
Roshan, S., T. DeVries, J. Wu, S. John, and T. Weber. 2020. Reversible scavenging traps hydrothermal iron in the deep ocean. *Earth and Planetary Science Letters* 542:116297, https://doi.org/10.1016/j.epsl.2020.116297.
Ruacho, A., R.M. Bundy, C.P. Till, S. Roshan, J. Wu, and K.A. Barbeau. 2020. Organic dissolved copper speciation across the US GEOTRACES equatorial Pacific zonal transect GP16. *Marine Chemistry* 225:103841, https://doi.org/10.1016/j.marchem.2020.103841.
Saito, M.A., A.E. Noble, A. Tagliabue, T.J. Goepfert, C.H. Lamborg, and W.J. Jenkins. 2013. Slow-spreading submarine ridges in the South Atlantic as a significant oceanic iron source. *Nature Geoscience* 6:775–779, https://doi.org/10.1038/ngeo1893.
Sander, S.G., and A. Koschinsky. 2011. Metal flux from hydrothermal vents increased by organic complexation. *Nature Geoscience* 4:145–150, https://doi.org/10.1038/ngeo1088.
Sedwick, P.N., B.M. Sohst, S.J. Ussher, and A.R. Bowie. 2015. A zonal picture of the water column distribution of dissolved iron(II) during the U.S. GEOTRACES North Atlantic transect cruise (GEOTRACES GA03). *Deep Sea Research Part II* 116:166–175, https://doi.org/10.1016/j.dsr2.2014.11.004.
Sieber, M., T.M. Conway, G. de Souza, C.S. Hassler, M.J. Ellwood, and D. Vance. 2021. Isotopic fingerprinting of biogeochemical processes and iron sources in the iron-limited surface Southern Ocean. *Earth and Planetary Science Letters* 567:116967, https://doi.org/10.1016/j.epsl.2021.116967.
Sieber, M., N.T. Lanning, X. Bian, S.-C. Yang, S. Takano, Y. Sohrin, T.S. Weber, J.N. Fitzsimmons, S.G. John, and T.M. Conway. 2023. The importance of reversible scavenging for the marine Zn cycle evidenced by the distribution of zinc and its isotopes in the Pacific Ocean. *Journal of Geophysical Research: Oceans* 128(4):e2022JC019419, https://doi.org/10.1029/2022JC019419.
Spiess, F.N., K.C. Macdonald, T. Atwater, R. Ballard, A. Carranza, D. Cordoba, C. Cox, V.D. Garcia, J. Francheteau, J. Guerrero, and others. 1980. East Pacific Rise: Hot springs and geophysical experiments. *Science* 207(4438):1,421–1,433, https://doi.org/10.1126/science.207.4438.1421.
Stichel, T., K. Pahnke, B. Duggan, S.L. Goldstein, A.E. Hartman, R. Paffrath, and H.D. Scher. 2018. TAG plume: Revisiting the hydrothermal neodymium contribution to seawater. *Frontiers in Marine Science* 5:96, https://doi.org/10.3389/fmars.2018.00096.
Tagliabue, A., L. Bopp, J.-C. Dutay, A.R. Bowie, F. Chever, P. Jean-Baptiste, E. Bucciarelli, D. Lannuzel, T. Remenyi, G. Sarthou, and others. 2010. Hydrothermal contribution to the oceanic dissolved iron inventory. *Nature Geoscience* 3(4):252–256, https://doi.org/10.1038/ngeo818.
Tagliabue, A., and J. Resing. 2016. Impact of hydrothermalism on the ocean iron cycle. *Philosophical Transactions of the Royal Society A* 374(2081), https://doi.org/10.1098/rsta.2015.0291.
Tagliabue, A., A.R. Bowie, T. Holmes, P. Latour, P. van der Merwe, M. Gault-Ringold, K. Wuttig, and J.A. Resing. 2022. Constraining the contribution of hydrothermal iron to Southern Ocean export production using deep ocean iron observations. *Frontiers in Marine Science* 9:754517, https://doi.org/10.3389/fmars.2022.754517.
Tilliette, C., V. Taillandier, P. Bouruet-Aubertot, N. Grima, C. Maes, M. Montanes, G. Sarthou, M.E. Vorrath, V. Arnone, M. Bressac, and others. 2022. Dissolved iron patterns impacted by shallow hydrothermal sources along a transect through the Tonga-Kermadec Arc. *Global Biogeochemical Cycles* 36(7), https://doi.org/10.1029/2022GB007363.
Toner, B.M., M.A. Marcus, K.J. Edwards, O. Rouxel, and C.R. German. 2012. Measuring the form of iron in hydrothermal plume particles. *Oceanography* 25(1):209–212, https://doi.org/10.5670/oceanog.2012.19.
Tonnard, M., H. Planquette, A.R. Bowie, P. van der Merwe, M. Gallinari, F. Desprez de Gésincourt, Y. Germain, A. Gourain, M. Benetti, G. Reverdin, and others. 2020. Dissolved iron in the North Atlantic Ocean and Labrador Sea along the GEOVIDE section (GEOTRACES section GA01). *Biogeosciences* 17(4):917–943, https://doi.org/10.5194/bg-17-917-2020.
Torres-Rodriguez, N., J. Yuan, S. Petersen, A. Dufour, D. González-Santana, V. Chavagnac, H. Planquette, M. Horvat, D. Amouroux, C. Cathalot, and others. 2024. Mercury fluxes from hydrothermal venting at mid-ocean ridges constrained by measurements. *Nature Geoscience* 17(1):51–57, https://doi.org/10.1038/s41561-023-01341-w.
Trocine, R.P., and J.H. Trefry. 1988. Distribution and chemistry of suspended particles from an active hydrothermal vent site on the Mid-Atlantic Ridge at 26°N. *Earth and Planetary Science Letters* 88(1):1–15, https://doi.org/10.1016/0012-821X(88)90041-6.
Valk, O., M.M. Rutgers van der Loeff, W. Geibert, S. Gdaniec, M.J.A. Rijkenberg, S.B. Moran, K. Lepore, R.L. Edwards, Y. Lu, and V. Puigcorbé. 2018. Importance of hydrothermal vents in scavenging removal of ^{230}Th in the Nansen Basin. *Geophysical Research Letters* 45(19):10,539-10,548, https://doi.org/10.1029/2018GL079829.
van Hulten, M., R. Middag, J.-C. Dutay, H. de Baar, M. Roy-Barman, M. Gehlen, A. Tagliabue, and A. Sterl. 2017. Manganese in the west Atlantic Ocean in the context of the first global ocean circulation model of manganese. *Biogeosciences* 14(5):1,123–1,152, https://doi.org/10.5194/bg-14-1123-2017.
van Hulten, M., J.C. Dutay, and M. Roy-Barman. 2018. A global scavenging and circulation ocean model of thorium-230 and protactinium-231 with improved particle dynamics (NEMO–ProThorP 0.1). *Geoscientific Model Development* 11(9):3,537–3,556, https://doi.org/10.5194/gmd-11-3537-2018.
Von Damm, K.L., J.M. Edmond, B. Grant, C.I. Measures, B. Walden, and R.F. Weiss. 1985. Chemistry of submarine hydrothermal solutions at 21°N, East Pacific Rise. *Geochimica et Cosmochimica Acta* 49:2,197–2,220, https://doi.org/10.1016/0016-7037(85)90222-4.
Von Damm, K. 1995. Controls on the chemistry and temporal variability of seafloor hydrothermal fluids. Pp. 222–247 in *Seafloor Hydrothermal Systems: Physical, Chemical, Biological, and Geological Interactions*. Geophysical Monograph Series, vol. 91, S.E. Humphris, R.A. Zierenberg, L.S. Mullineaux, and R.E. Thomson, eds, American Geophysical Union, Washington DC, https://doi.org/10.1029/GM091p0222.
Wang, H., W. Wang, M. Liu, H. Zhou, M.J. Ellwood, D.A. Butterfield, N.J. Buck, and J.A. Resing. 2022. Iron ligands and isotopes in hydrothermal plumes over backarc volcanoes in the Northeast Lau Basin, Southwest Pacific Ocean. *Geochimica et Cosmochimica Acta* 336:341–352, https://doi.org/10.1016/j.gca.2022.09.026.
Whitmore, L.M., A.M. Shiller, T.J. Horner, Y. Xiang, M.E. Auro, D. Bauch, F. Dehairs, P.J. Lam, J. Li, M.T. Maldonado, and others. 2022. Strong margin influence on the Arctic Ocean barium cycle revealed by pan-Arctic synthesis. *Journal of Geophysical Research: Oceans* 127(4):e2021JC017417, https://doi.org/10.1029/2021JC017417.
Wu, J., S. Roshan, and G. Chen. 2014. The distribution of dissolved manganese in the tropical-subtropical North Atlantic during US GEOTRACES 2010 and 2011 cruises. *Marine Chemistry* 166:9–24, https://doi.org/10.1016/j.marchem.2014.08.007.
Xu, H., and T. Weber. 2021. Ocean dust deposition rates constrained in a data-assimilation model of the marine aluminum cycle. *Global Biogeochemical Cycles* 35(9):e2021GB007049, https://doi.org/10.1029/2021GB007049.
Yucel, M., A. Gartman, C.S. Chan, and G.W. Luther. 2011. Hydrothermal vents as a kinetically stable source of iron-sulphide-bearing nanoparticles to the ocean. *Nature Geoscience* 4:367–371, https://doi.org/10.1038/ngeo1148.
Zhang, R., L. Jensen, J. Fitzsimmons, R.M. Sherrell, P. Lam, Y. Xiang, and S. John. 2021. Iron isotope biogeochemical cycling in the western Arctic Ocean. *Global Biogeochemical Cycles* 35(11), https://doi.org/10.1029/2021GB006977.
Zheng, L., T. Minami, W. Konagaya, C.-Y. Chan, M. Tsujisaka, S. Takano, K. Norisuye, and Y. Sohrin. 2019. Distinct basin-scale-distributions of aluminum, manganese, cobalt, and lead in the North Pacific Ocean. *Geochimica et Cosmochimica Acta* 254:102–121, https://doi.org/10.1016/j.gca.2019.03.038.

ACKNOWLEDGMENTS

We thank members of the leadership of the international GEOTRACES program for their vision for studying the geochemistry of hydrothermal plumes, in particular the chief scientists of the hydrothermal GEOTRACES studies cited in this review. We also thank Natalie Renier for her help in designing Figure 1. JMS was funded by NSF OPP-1941308, and JNF was funded by NSF OCE-1851078, OCE-2023206, and OCE- 2049241. The international GEOTRACES program is possible in part thanks to the support from the US National Science Foundation (Grant OCE-2140395) to the Scientific Committee on Oceanic Research (SCOR).

AUTHORS

Jessica N. Fitzsimmons (jessfitz@tamu.edu) is Associate Professor, and **Janelle M. Steffen** is a graduate student, both in the Department of Oceanography, Texas A&M University, College Station, TX, USA.

ARTICLE CITATION

Fitzsimmons, J.N., and J.M. Steffen. 2024. The "net" impact of hydrothermal venting on oceanic elemental inventories: Contributions to plume geochemistry from the international GEOTRACES program. *Oceanography* 37(2):102–115, https://doi.org/10.5670/oceanog.2024.421.

COPYRIGHT & USAGE